TECTONICS, VOL. 11, NO. 1, PAGES 36-46, FEBRUARY 1992

STRESS MAGNITUDE, STRAIN RATE, AND RHEOLOGY OF EXTENDED MIDDLE CONTINENTAL CRUST INFERRED FROM QUARTZ GRAIN SIZES IN THE WHIPPLE MOUNTAINS, CALIFORNIA

Bradley R. Hacker
Department of Geology, Stanford University, Stanford, California

An Yin and John M. Christie
Department of Earth and Space Sciences, University of California, Los Angeles

G.A. Davis
Department of Geology, University of Southern California, Los Angeles

Abstract. Knowledge of the magnitude of differential stress and strain rate during the formation of mylonitic shear zones in metamorphic core complexes provides constraints on the mechanical behavior of the middle continental crust during extension. We analyzed the differential flow stress during the mylonitization of quartzofeldspathic rocks in the Whipple Mountains, California, using grain-size piezometers and kinetic laws for grain growth. Mylonitic gneisses collected from two widely separated transects have grain sizes that cluster in a range from 32 to 61 μm. Analysis of grain growth kinetics indicates that mylonitization of the gneisses continued during cooling to temperatures ≤500°C, compatible with estimates from two-feldspar thermometry. Quartz grain-size piezometers suggest that the mylonitization occurred under differential stresses (σ_1-σ_3) of ~40–150 MPa, or maximum shear stresses of 20–75 MPa. Extrapolation of quartzite flow laws to 500°C indicates that the mylonitization occurred at strain rates faster than 10^{-14} s^{-1}. These estimates suggest that the mylonitic zone within the Whipple Mountains had an effective viscosity of the order of $10^{18\pm4}$–$10^{20\pm4}$ Pa s. These low viscosities and rapid strain rates, combined with seismic reflection data showing that continental crust is layered, suggest that more realistic physical models of extension of the continental lithosphere should treat the lithosphere as a heterogeneous distribution of high-viscosity regions separated by low-viscosity zones.

INTRODUCTION

Our knowledge of the rheology of the continental lithosphere has improved greatly in the past decade. Earth scientists no longer treat the continents as plates with a uniform strength as we did 20 years ago. Rather, a "layered" model for the continental lithosphere—composed of brittle layers with pressure-dependent strength and ductile layers with temperature-dependent strength—has been widely used [Brace and Kohlstedt, 1980; Sibson, 1982; Chen and Molnar, 1983]. The foundation of this rheological model consists of experimentally derived constitutive relationships for frictional sliding of rocks and dislocation creep and dynamic recrystallization of quartzite and dunite. The "layer" model is used to explain a wide range of phenomena, including the distribution of seismicity as a function of depth [Sibson, 1982; Chen and Molnar, 1983], potential delamination of the continental mantle lithosphere [e.g., Bird, 1979], and the development of crustal-scale shear zones in extensional and contractional orogens [e.g., Davis et al., 1986; Kulik and Schmidt, 1988; Ord and Hobbs, 1989]. This model also provides the basis for geodynamic modeling of deformation of the continental lithosphere [e.g., Lynch and Morgan, 1987; Sonder et al., 1987; Bird, 1989]. To construct a well-constrained rheological model, however, three fundamental parameters—temperature, strain rate, and stress—must be determined for the situation of interest. These parameters vary greatly, and determination of their values for different rock types and different tectonic settings remains a substantial challenge to geologists. Thermal gradients have been investigated through thermal modeling, direct heat-flow measurements, and fission track and $^{40}Ar/^{39}Ar$ studies [e.g., Sclater et al., 1980; Zeitler et al., 1982; Copeland et al., 1987; Furlong and Chapman, 1987]. They vary from ~7°C km^{-1} in subduction zones [e.g., X. Wang et al., 1989] to ~30°C km^{-1} in extensional areas such as the present Basin and Range province [Lachenbruch and Sass, 1977]. The assumed and inferred strain rates in different tectonic settings vary from 10^{-11} s^{-1} to 10^{-16} s^{-1} [Sibson, 1982; Chen and Molnar, 1983; Sonder et al., 1987]. Estimates of the magnitude of stress also vary from ~1 MPa to ~200 MPa [e.g., Goetze, 1975; Twiss, 1977; Kanamori, 1980; Ord and Christie, 1984; Carter and Tsenn, 1987; McNutt, 1987; Molnar and England, 1990]. Because stress, strain rate, and thermal gradient may vary over such a wide range (several orders of magnitude), construction of realistic rheological models for the deformation of continental lithosphere is difficult. Meaningful models can be produced only if values for the thermal gradient, stress magnitude, and strain rate can be more tightly constrained for a given region. Studies of Cordilleran metamorphic core complexes provide an opportunity to constrain the values of these three variables during extension of the continental lithosphere.

The purpose of this paper is to use theoretically derived and experimentally calibrated microstructural piezometry of quartz to infer the differential stress during the mylonitization of quartzofeldspathic rocks along the mid-Tertiary mylonitic shear zone exposed in the Whipple Mountains. Piezometry is the measurement of differential stress; for a brief discussion of piezometry and its application to rocks, see Hacker et al. [1990]. The inferred flow stress (equal to differential stress) is used to calculate the strain rate during mylonitization by applying experimental flow laws for quartzite. The effective viscosity of the mylonitic shear zone is also estimated, and implications of the inferred shear stress and effective viscosity in mechanical and regional tectonic models for the formation of the Cordilleran core complexes are discussed.

Cordilleran metamorphic core complexes and detachment fault terranes are distinctive structural associations of Tertiary age and extensional origin. They have been intensively studied in the past decade [e.g., Crittenden et al.,

Paper number 91TC01291.
0278-7407/92/91TC-01291$10.00

1980; Frost and Martin, 1982; Lister and Snoke, 1984; Coney and Harms, 1984; Davis and Lister, 1988; Lister and Davis, 1989]. Core complexes are good places to study the rheology of continental crust during extension for the following reasons. (1) Quartzofeldspathic rocks are the dominant lithology of mylonitic shear zones in some metamorphic core complexes. This allows application of the considerable experimental data available on the deformation and annealing of quartzose rocks. (2) Kinematic models for the development of the mylonitic shear zones are well developed [Wernicke, 1985; Davis et al., 1986; Gans et al., 1989], providing a conceptual framework for understanding how the deformation microstructures are related to the cooling and depressurization history of the rocks. (3) The age of detachment faulting and mylonitization of lower plate mylonitic shear zones are constrained in a few core complexes through detailed geochronologic studies. In addition, application of fission track and $^{40}Ar/^{39}Ar$ thermochronology allows reconstruction of cooling histories of the mylonitic rocks during their transport to Earth's surface (see summaries by Davis [1988] for the Whipple Mountains; Lee and Sutter [1991] for the Snake Range; and Snoke and Miller [1988] for the Ruby Mountains). 4) The temperatures and depths at which the mylonitic rocks formed have been estimated from thermobarometry [e.g., Anderson, 1988], reflection seismology [e.g., Frost and Okaya, 1987], and paleo-depth reconstructions [e.g., Miller et al., 1983; Howard et al., 1982].

Another important aspect of this study is that it provides critical information about mechanical conditions in the middle and lower crust. Recent studies in the North American Cordillera suggest that dynamic processes within ductilely deformed middle to lower continental crust played an important role in mid-Tertiary core-complex and late Cenozoic Basin and Range extension. This is evident from the widespread, ductilely deformed middle crustal mylonitic rocks exposed in the lower plates below many major detachment faults [e.g., Anderson, 1988; Snoke and Miller, 1988], and from correlations of exposed mylonitic zones with reflections in seismic profiles [e.g., Frost and Okaya, 1987; Valasek et al., 1989]. Coney and Harms [1984] suggested that the initiation of core-complex extension was related to gravitational spreading of a thick crustal root in the North American Cordillera produced during the Laramide and Sevier orogenies. Bird [1991] showed that the rate of ductile flow in a thickened middle and lower crust due to gravitational spreading depends strongly on the thermal regime of the lithosphere. On the basis of the correlation between the mylonitic gneisses exposed in southeastern California and western Arizona with the middle/lower crustal seismic reflectors, Yin [1989] suggested that ductile flow in the middle and lower crust produced shear stresses acting on the base of the upper crust that controlled the stress distribution in the elastic–brittle upper crust. In particular, low (tens of bars) and high (hundreds of bars) basal shear stresses can produce distinctive stress distributions, which in turn produce different predicted fault patterns. The knowledge of the magnitude of differential stress in the middle and lower crust during extension thus places constraints on possible stress distributions in the upper crust.

THE WHIPPLE MOUNTAINS

The Whipple Mountains core complex of southeastern California (Figure 1) is commonly cited as a type example of a metamorphic core complex, and extensive structural, geochronological, and thermobarometric studies have been conducted there [e.g., Davis et al., 1980, 1982, 1986; Anderson and Rowley, 1981; Wright et al., 1986; Anderson, 1988;

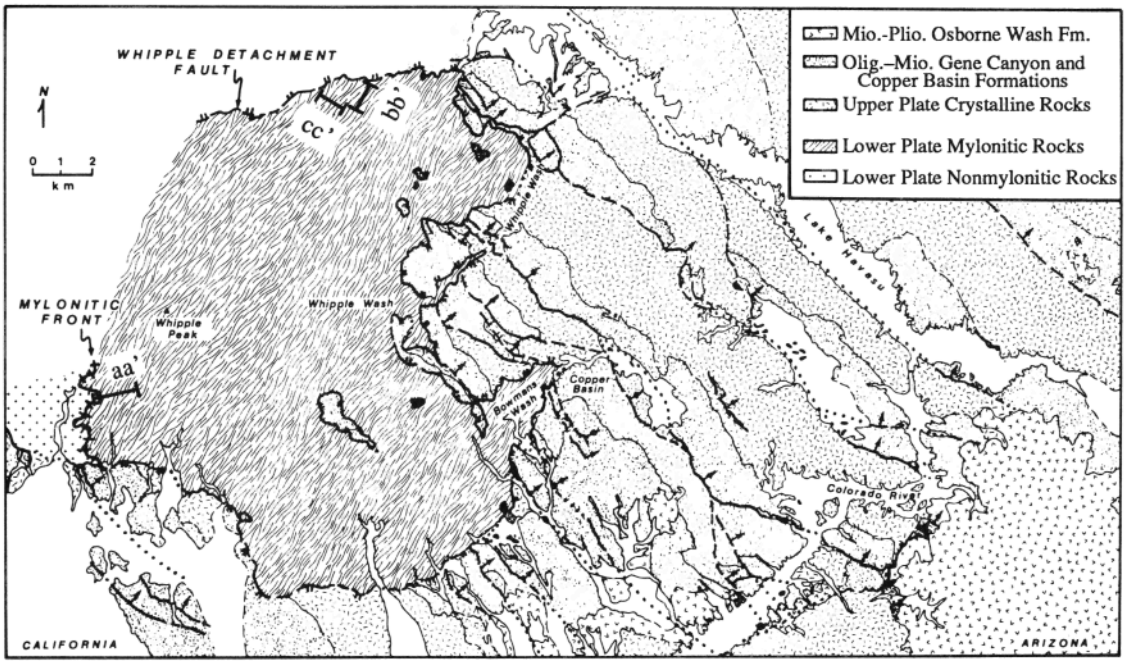

Fig. 1. Geologic map of the Whipple Mountains [after Anderson et al., 1979], including locations of samples collected in this study. Transects a-a', b-b', and c-c' comprise samples Wh-1 to Wh-13, Wh-20 to Wh-31, and Wh-40 to Wh-57, respectively.

Davis, 1988; Davis and Lister, 1988; Lister and Davis, 1989]. Figure 1 is a simplified geologic map of the central and eastern Whipple Mountains that illustrates the major structural features of the range. The low-angle Whipple Mountains detachment fault divides the crust into upper and lower plates. Crystalline rocks of the lower plate are exposed in the core of a complex dome, and are separated into two structural domains by the Whipple mylonitic front. The mylonitic front is a gradational SW-dipping contact between Tertiary mylonitic gneisses and structurally higher, generally equivalent crystalline rocks that escaped mylonitization. It varies from as narrow as several meters to a zone ~100 m wide.

The significance of the mylonitic front is that it marks a major structural boundary of Tertiary age within the crust (Figure 2). It is the upper limit of a greater than 3.5-km-thick sequence of lower plate mylonitic gneisses formed by intracrustal ductile flow [Davis and Lister, 1988]. The mylonitic gneisses are characterized by a gently arched SW- to NE-dipping foliation and a consistent NE-SW-trending stretching lineation. Above the mylonitic front, Precambrian gneisses and interlayered amphibolites have a steep, NE-striking nonmylonitic foliation. This premylonitic foliation is both rotated and transposed at the mylonitic front [Davis et al., 1980]. Directly below the mylonitic front, isolated relict domains of steeply dipping Precambrian gneisses intruded by Cretaceous sills are preserved within the less steeply dipping mylonitic sequence, especially between mylonitized Cretaceous plutonic sheets [Davis, 1988, Figure 10].

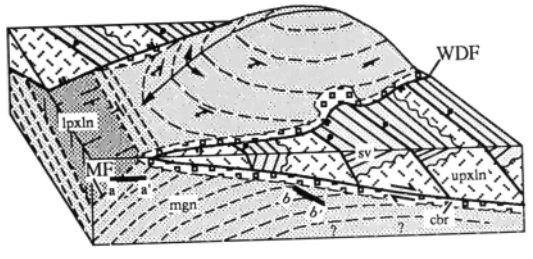

Fig. 2. Vertically exaggerated representation of the Whipple Mountains core complex, showing diagrammatic structural positions of samples collected in this study. Abbreviations are WDF, Whipple detachment fault; MF, mylonitic front; lpxln, lower plate crystalline rocks; mgn, undifferentiated mylonitic rocks; cbr, chloritic breccias; upxln, upper plate crystalline rocks; sv, Miocene sedimentary and volcanic rocks.

Seismic reflection profiles by CALCRUST southwest of the Whipple Mountains show a zone of high reflectivity beneath the seismically transparent uppermost crust beginning at ~8–12 km depth and continuing to ~21 km. The base of the crust is interpreted in the CALCRUST profile to be at ~28 km [C.-Y. Wang et al., 1989]. Davis [1988] and Davis and Lister [1988] suggest that this zone of reflectivity correlates with the mylonitic rocks in the Whipple Mountains. As proposed by Lister and Davis [1989] and Yin [1989], this correlation implies that the subhorizontal base of the upper crust was the locus of a downward transition to ductile deformation prior to and during the formation of the Whipple detachment fault. For example, shearing at the base of the upper crust induced by directed ductile flow in the middle and lower crust may have been responsible for the low-angle normal faults in the region [Yin, 1989].

A Tertiary (26±5 Ma) age for mylonitization in the Whipple Mountains has been documented by Wright et al. [1986]. Thermobarometric studies by Anderson [1988] indicate that mylonitization occurred at temperatures increasing with depth from about 460° to 535°C at an average pressure of ~460 MPa. $^{40}Ar/^{39}Ar$ plateau ages of metamorphic subcalcic hornblende and muscovite in mylonitized rocks [DeWitt et al., 1986] indicate cooling of the mylonitic gneisses from 525±75°C (range of ^{40}Ar retention temperatures of hornblende at cooling rates >10°C m.y.$^{-1}$ Harrison, 1981] at 19.2±0.2 Ma ago to 350°±25°C (^{40}Ar retention temperature of muscovite; McDougall and Harrison, 1988]) at 18.0±0.1 Ma; this implies a cooling rate of 146^{+159}_{-96}°C m.y.$^{-1}$. Fission track ages of three zircons, one apatite, and one sphene crystal vary from 17.9 to 20.4 Ma, with an overlap of error bars between 18.4 and 19.5 Ma, indicating that the rocks cooled to less than 70°–130°C (maximum closure temperature of apatite; Dokka et al., 1986) by 17.9 Ma [Dokka and Lingrey, 1979]. The $^{40}Ar/^{39}Ar$ and fission track data collectively imply that rocks from the Whipple Mountains cooled from 525°±75°C to <130°C at rates greater than 200°C m.y.$^{-1}$ over a period of ~1.3 m.y. This cooling rate is rather uncertain because (1) without detailed characterization of the hornblende microstructure and age spectrum, its ^{40}Ar retention temperature is poorly known; and (2) deformation could have altered the hornblende or muscovite age spectra; (3) the samples may have moved closer together after they cooled below their Ar retention temperatures [Hacker, 1991] and may reflect spatially separated thermal events. These thermochronologic data in conjunction with the probable 35–40 km displacement of a Tertiary dike swarm indicate that the midcrustal mylonitic gneisses were carried rapidly upward in the footwall of the Whipple Mountains detachment fault system between 20 and 18 Ma [Davis and Lister, 1988; Davis, 1988]. Both the mylonitic gneisses, with their NE–SW stretching lineation, and the somewhat younger brittle detachment faults, with their NE–SW direction of displacement, are believed to be expressions of profound mid-Tertiary extension of the continental lithosphere.

SAMPLE COLLECTION

Samples for this study were collected from two transects in the Whipple Mountains: one directly beneath the Whipple detachment fault along the "Powerline" road on the north side of the range and one directly below the mylonitic front on the southwest side of the range (Figures 1 and 2). Samples from the north side of the range are structurally lower than those from the southwest side with respect to the mylonitic front (Figure 2).

On the north side of the range, mylonitic rocks of the lower plate consist of interlayered biotite quartzofeldspathic gneiss, granitic augen gneiss, and amphibolite [Davis et al., 1980]. The degree of mylonitization is spatially variable; in layers that contain abundant quartz and mica the mylonitic foliation and stretching lineation are strongly developed, whereas feldspar- and amphibole-rich layers are less foliated and weakly lineated. Twenty-five samples of quartzofeldspathic gneiss were collected along a ~1000-m east–west transect at approximately 115°28'W and 40°41.5'N. The gneissic foliation comprises alternating

quartzose layers (10–50 vol %) and feldspathic layers. Feldspar crystals occur as isolated porphyroclasts and in folia that extend outward from porphyroclasts. Feldspar porphyroclasts are typically cracked; local twins and undulatory extinction reflect some dislocation mobility, perhaps during early high-temperature deformation. Feldspar crystals in folia are a few micrometers in diameter and are cataclastic fragments, rather than recrystallized grains, as indicated by their angular shape and grain-scale cracks. Epidote, muscovite, chlorite, sphene, calcite, and ilmenite or magnetite altered to hematite, are common accessory minerals.

The quartz within the gneiss occurs in discontinuous globular patches as large as 1 cm, and in continuous layers ranging in thickness from 3 cm to ~1 mm. Some of these layers may originally have been veins, but they are now transposed parallel to the foliation. The quartz textures in these samples are variable. Some specimens contain relict igneous grains with continuous undulatory extinction and only minor grain-boundary bulges or subgrains. More-deformed specimens contain ribbon grains with variably developed deformation lamellae and stronger undulatory extinction (Figure 3a). Other samples are composed of equant to subequant recrystallized grains. Quartz lattice preferred orientations are often well developed, as indicated by the uniformity of interference colors produced by crossed polarizers and a gypsum plate. The variation in the degree of recrystallization may indicate that the deformation was not

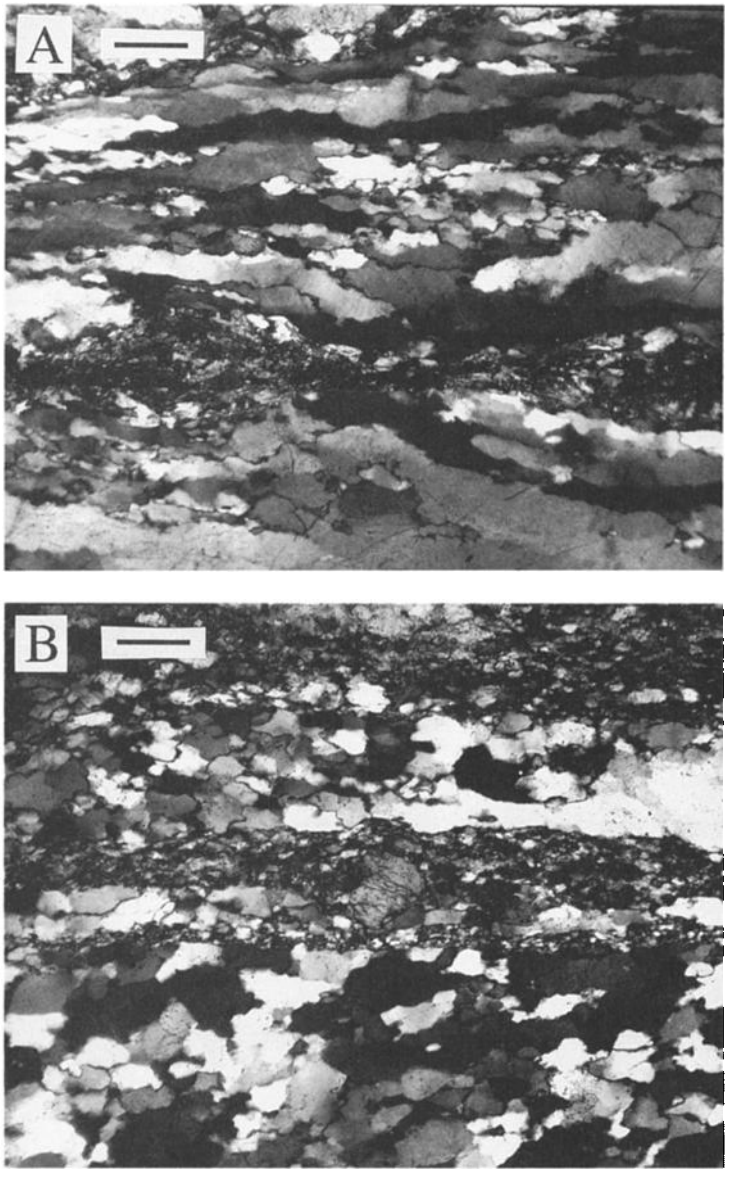

Fig. 3. Cross-polarized optical micrographs of mylonitic granitoid textures. (a) Partially recrystallized mylonitic rock with ribbon grains containing sub-basal deformation lamellae (sample Wh-10). (b) Completely recrystallized quartz layers and cataclastic feldspar layers (sample Wh-54). Scale in each micrograph is 100 μm.

uniform throughout the mylonitic shear zone. Only samples composed of recrystallized grains of relatively uniform size were considered in the following analysis.

In the southwestern portion of the Whipple Mountains, the mylonitic front is well developed and exposed. Fourteen samples were collected along a 930-m ENE transect (Figure 1). In all samples, the quartz is equant to subequant recrystallized grains with moderate to slight undulatory extinction, variably developed lattice preferred orientation, and relatively straight grain boundaries (Figure 3b). The plagioclase crystals are anhedral, fractured augen.

GRAIN SIZE DETERMINATION

The recrystallized grain sizes were measured in pure quartz layers by the mean linear intercept method described by Hacker et al. [1990]. The actual grain diameter, $\bar{D}$, is equal to 3/2 $\bar{L}$, the measured mean grain size. Samples with relatively uniform recrystallized grains from the north side of the range have grain sizes of 53–162 μm (Table 1; Figure 4). The rocks collected directly below the mylonitic front on the southwest side contain grains with a more restricted range of sizes from 32 to 61 μm (Table 1). This suggests that the differential stresses, thermal histories, and/or grain growth histories may have been different in the two locations. Because postdeformational grain growth may have occurred under low deviatoric or hydrostatic stress, the measured grain sizes may be larger than the grain sizes developed during the mylonitization.

No systematic correlations among the mean grain size, the standard deviation of grain size, the aspect ratios of quartz crystals, the amount of quartz in the samples, the size of the quartzose layers in the samples, the degree of lattice preferred orientation, or the development of undulatory extinction were found in the mylonitic gneisses. The lack of any correlation between the grain size and other features of these samples gives us confidence that the grain size is not influenced systematically by the average amount of quartz in the samples or the thickness of the quartzose layers in which the grains were measured.

POSTDEFORMATIONAL ANNEALING

Grain sizes that develop during deformation can increase during postdeformational annealing (after removal of deviatoric stress), particularly if the annealing period is lengthy, the annealing begins at high temperatures [Twiss, 1977], or the grain size is small. Invariably, grains are larger after annealing than they were during deformation, and the larger, annealed grain size leads to an underestimate of the actual flow stress. The kinetics of grain growth in quartzite as a function of pressure and temperature have been determined [Tullis and Yund, 1982; Pierce and Christie, 1987], and the effect of grain growth during annealing is evaluated in this section.

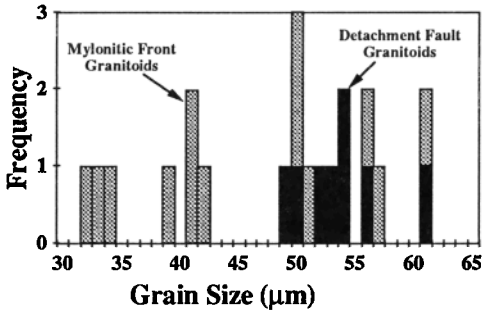

Fig. 4. Histogram of measured grain sizes from samples with homogeneous textures composed of subequant grains.

TABLE 1. Measurements From Samples With Relatively Uniform, Subequant Recrystallized Grains

Sample	N	$\bar{D}$, μm	Grain Shape
Below Detachment Fault on North Side of Range			
Wh-5	728	61±04	0.7 : 1.0 : 1.2
Wh-6	872	53±06	0.7 : 1.0 : 1.6
Wh-8	816	56±04	0.8 : 1.0 : 1.1
Wh-20	736	89±06	0.8 : 1.0 : 1.0
Wh-23	899	106±07	0.7 : 1.0 : 1.5
Wh-27	717	134±11	0.8 : 1.0 : 1.5
Wh-29	598	162±20	0.9 : 1.0 : 1.0
Wh-30	824	115±09	1.0 : 1.0 : 1.3
Beneath Mylonitic Front on Southwest Side of Range			
Wh-40	888	51±04	1.0 : 1.0 : 1.2
Wh-41	815	56±04	0.7 : 1.0 : 1.2
Wh-42	1168	39±03	0.8 : 1.0 : 1.1
Wh-43	1096	41±03	0.9 : 1.0 : 1.0
Wh-44	1318	34±04	0.7 : 1.0 : 1.1
Wh-45	738	61±04	1.0 : 1.0 : 1.1
Wh-47	1112	41±03	0.7 : 1.0 : 1.1
Wh-48	1069	42±03	0.8 : 1.0 : 1.1
Wh-49	1358	33±03	0.7 : 1.0 : 1.0
Wh-51	1406	32±02	0.7 : 1.0 : 1.1
Wh-53	897	51±03	0.8 : 1.0 : 1.4
Wh-54	893	50±03	0.8 : 1.0 : 1.2
Wh-57	787	57±05	0.6 : 1.0 : 1.1

N is the number of measured grains.

Estimates of the peak temperature and pressure during mylonitization, determined from two-feldspar thermometry and barometry based on the Si content of muscovite, are ~460°C and ~460 MPa for rocks at shallow levels beneath the Whipple detachment fault and ~535°C at structural levels ~2.5 km deeper [Anderson, 1988; Anderson et al., 1988]. Consideration of the grain growth kinetics of quartz aggregates suggests mylonitization temperatures that are compatible with these estimates. The average grain sizes of recrystallized quartz in the mylonitic gneisses cluster at 37 and 55 μm (Figure 4). From the kinetic laws for the grain growth of quartz [Tullis and Yund, 1982; Pierce and Christie, 1987], we calculated by numerical integration the grain growth history for grains with a final diameter of 37 and 55 μm developed during cooling at constant rates (Figure 5). The calculation involves the following summation, each term of which describes the grain growth from an initial grain size $\bar{L}_{i-1}$ to a final grain size $\bar{L}_i$ over the time interval t (s) at temperature T_i (K):

$$\bar{L} = \sum_{i=1}^{n} \sqrt{c(T_i)t + L_{i-1}^2} \quad ; \; c(T_i) = c_o \exp\left(-(H+PV^*)/RT_i\right)$$

Where $c_o = 7.47 \times 10^{-4}$ m^2 s^{-1}, H = 281 kJ/mol, $V^* = -1.86 \times 10^{-8}$ m^3 mol^{-1}, and R is the gas constant. The value of n (number of summed terms) is equal to the number of steps

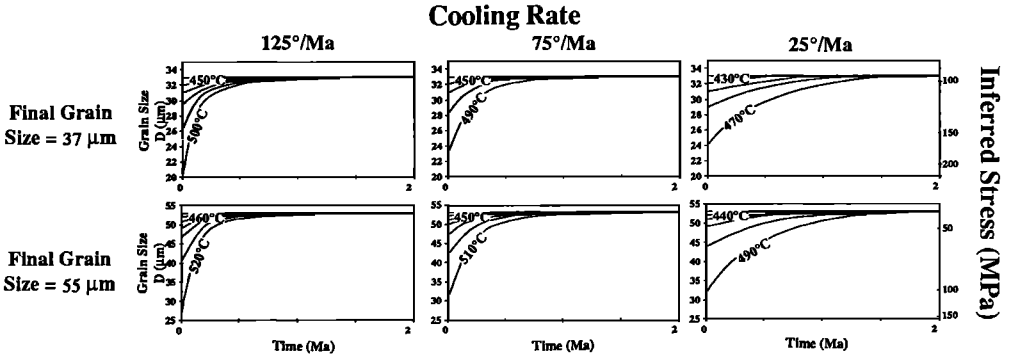

Fig. 5. Grain growth paths to reach final grain sizes of $\bar{D}$ = 37 and 55 μm at various constant cooling rates. This assumption of constant cooling rate is a more precise constraint than the assumption of exponential conductive cooling, because heat is not lost as rapidly initially.

required to reduce the initial temperature to 0°C for a given cooling rate and chosen time interval t. The quartz grain growth experiments on which our calculations are based were conducted with 1 wt % water added to promote grain growth. The samples were damp on removal of their silver jackets after the experiments, so that the water pressure was equal to the confining pressure during the experiments. These calculations represent the extreme case where $P_{H_2O} = P_{total}$ during the cooling history. A pressure of 0.46 GPa was used based on work of Anderson [1988].

Figure 5 shows several grain growth paths for cooling from different temperatures at linear rates of 25, 75, and 125°C m.y.$^{-1}$. These cooling rates are conservatively slower than those given by $^{40}Ar/^{39}Ar$ and fission track data, because of the previously mentioned uncertainties regarding the cooling rates. The paths were calculated by assuming that steady state deformation during mylonitization produced a grain size controlled by the differential stress; then the mylonitization ceased instantaneously and was followed by annealing during hydrostatic cooling. Although this assumption grossly oversimplifies the likely stress and temperature history, data for more sophisticated modeling are not presently available.

Grains of 37-μm diameter can form during annealing from any initial grain size smaller than 37 μm. At ≤450°C, 37-μm grains cooled at 125°C m.y.$^{-1}$ do not grow; this temperature is symbolized as T_a, the "annealing blocking temperature," for this grain size and cooling rate. During cooling from 500°C, grains that were initially 26 μm grow to a final grain size of 37 μm in less than 2 m.y. At temperatures ≥510°C, grains grow rapidly to more than 37 μm, regardless of the initial grain size. This places an upper limit (T_{max}) on the temperature at the end of mylonitization of the 37-μm quartz aggregates of 500°C, based on grain growth kinetics. Thus 26 μm is the minimum grain size that could have resulted from mylonitization at 500°C (Figure 5).

Similar calculations and reasoning indicate that T_a=460°C and T_{max}=520°C for the mylonitic gneisses with a final grain size of 55 μm cooled at 125°C m.y.$^{-1}$. The minimum grain size that could have resulted from mylonitization of the 55-μm samples at 520°C is 28 μm (Figure 5).

DIFFERENTIAL STRESS DURING MYLONITIZATION

We used the recrystallized-grain-size piezometers of Twiss [1977, 1980], Mercier et al. [1977], and Koch [1983] (see Table 2 of Hacker et al. [1990]), to calculate the differential stress for each sample using our measured grain sizes (Table 2) and the grain sizes inferred from grain growth calculations. Mercier et al.'s [1977] piezometer is less precise because the grain-size measurements were made on 1–25 μm diameter grains in standard 30-μm-thick sections using transmitted light microscopy. We prefer the recrystallized-grain-size piezometer of Koch [1983], because it is based on combined data from experiments on "wet" and "dry" quartzite, flint, and novaculite, deformed over a wide range of pressures, temperatures, and strain rates, in solid-medium [Koch et al., 1989] and gas-medium apparatus [Mainprice, 1981]. Note, however, that the stresses inferred from the theoretical piezometer of Twiss [1977; 1980] are very similar for the majority of samples. Koch [1983] incorporated uncertainties in his and Mainprice's [1981] experimental measurements in his piezometer calibration; consequently, his piezometer yields uncertainties for the calculated differential stresses that include both the experimental calibration error and variance of the grain-size measurements. Koch's and Mainprice's data were acquired at stresses of ~50 to 2000 MPa, so that little or no extrapolation of their data to lower stresses is required [cf. Twiss, 1986]. Moreover, we used the same grain-size measurement technique that Koch used, so that our grain sizes are directly comparable to Koch's.

An important assumption is that the deformation mechanisms operative during the mylonitization were the same as those active during the experiments from which the piezometer was derived. In Koch's [1983] experiments on quartzite and novaculite, the recrystallized grain sizes were independent of strain rate, water content, temperature, initial grain size, and finite strain (beyond a certain critical strain), but this may be the result of a relatively restricted experimental range of strain rates, water contents, and temperatures. In rocks deformed under drier or wetter conditions, slower strain rates, and lower temperatures characteristic of natural deformation, the sizes of recrystallized grains may depend on these variables [e.g., Ord and Hobbs, 1986]. The deformation microstructures in Koch's samples are like those in the Whipple Mountains mylonitic rocks, although the natural rocks show less grain boundary recrystallization and greater development of subgrains relative to the experimental samples. This suggests that similar deformation mechanisms were operative, but that grain boundary mobility and dislocation recovery may have been greater in the natural samples.

TABLE 2. Calculated Differential Stresses

Sample	Grain Size $\bar{D}$, μm	Differential Stress (MPa) Twiss [1977, 1980]	Mercier et al. [1977]	Koch[1] [1983]
Below Detachment Fault on North Side of Range				
Wh-5	61±4	41^{+2}_{-1}	20^{+1}_{-1}	$34^{+4\ +17}_{-4\ -10}$
Wh-6	53±6	45^{+4}_{-3}	22^{+2}_{-1}	$43^{+10\ +28}_{-7\ -15}$
Wh-8	56±6	44^{+3}_{-3}	21^{+2}_{-1}	$39^{+8\ +25}_{-6\ -13}$
Wh-20	89±6	32^{+2}_{-1}	15^{+1}_{-0}	$18^{+2\ +8}_{-2\ -5}$
Wh-23	106±6	28^{+2}_{-1}	14^{+0}_{-1}	$13^{+2\ +6}_{-1\ -3}$
Wh-27	134±6	24^{+2}_{-1}	11^{+1}_{-0}	$9^{+1\ +4}_{-1\ -3}$
Wh-29	162±6	21^{+2}_{-1}	10^{+1}_{-1}	$6^{+2\ +4}_{-1\ -2}$
Wh-30	115±6	27^{+1}_{-1}	13^{+1}_{-1}	$12^{+1\ +5}_{-2\ -4}$
Beneath Mylonitic Front on Southwest Side of Range				
Wh-40	51±4	47^{+2}_{-3}	23^{+1}_{-1}	$46^{+7\ +25}_{-6\ -15}$
Wh-41	56±4	44^{+2}_{-2}	21^{+2}_{-1}	$39^{+5\ +20}_{-4\ -12}$
Wh-42	39±3	56^{+3}_{-3}	28^{+1}_{-2}	$72^{+10\ +41}_{-8\ -24}$
Wh-43	41±3	54^{+2}_{-3}	27^{+1}_{-2}	$66^{+9\ +37}_{-7\ -21}$
Wh-44	34±4	62^{+5}_{-5}	31^{+2}_{-3}	$91^{+21\ +65}_{-16\ -34}$
Wh-45	61±6	41^{+3}_{-2}	20^{+2}_{-1}	$34^{+6\ +20}_{-5\ -12}$
Wh-47	41±3	54^{+3}_{-2}	27^{+1}_{-2}	$66^{+9\ +37}_{-7\ -21}$
Wh-48	42±3	53^{+3}_{-2}	26^{+2}_{-1}	$64^{+18\ +34}_{-7\ -21}$
Wh-49	33±3	63^{+4}_{-4}	31^{+2}_{-2}	$96^{+16\ +60}_{-14\ -34}$
Wh-51	32±2	64^{+3}_{-2}	32^{+1}_{-1}	$101^{+11\ +55}_{-10\ -32}$
Wh-53	50±4	47^{+3}_{-2}	23^{+2}_{-1}	$47^{+7\ +27}_{-5\ -15}$
Wh-54	50±3	47^{+2}_{-2}	23^{+2}_{-1}	$47^{+6\ +24}_{-4\ -14}$
Wh-57	57±5	43^{+3}_{-2}	21^{+2}_{-1}	$38^{+6\ +21}_{-5\ -22}$

The uncertainties given are derived from (1) the standard deviation of the grain size (first or only +/- numbers), and from (2) the uncertainty of the grain size and the uncertainty of the piezometer calibration (second +/- numbers; for Koch [1983] only).

[1] Includes data from 6 experiments by Mainprice [1981].

Using the measured grain sizes (i.e., assuming no postdeformational annealing), differential stresses for the mylonitic gneisses from the north side of the range are 6–43 MPa, whereas grain sizes from samples near the mylonitic front suggest stresses as high as 101 MPa (Table 2). Note that the uncertainties of these values are in some cases a large fraction of the values themselves. Because the grain sizes may have increased during postdeformational annealing, these calculated differential stresses are lower limits to the stress during the mylonitization. Using the minimum pre-annealing grain size of 26 μm for a final 37 μm grain size (Figure 5), the stresses during mylonitization may have been as high as 143 MPa for rocks that cooled from 500°C at 125°C m.y.$^{-1}$.

EFFECT OF SLOWER COOLING

Only one rate of cooling, 125°C m.y.$^{-1}$, was considered in the previous discussion. This rate is quite fast and possibly inaccurate. Cooling rates of ~50°–100°C m.y.$^{-1}$ calculated for the Bitterroot mylonite [Hyndman and Myers, 1988] and Ruby Mountains core complex [Hacker et al., 1990] suggest that 125°C m.y.$^{-1}$ is probably too rapid. To explore the effects of variable cooling rates, we have calculated grain growth histories and implied pre-annealing stresses for cooling rates of 75°C m.y.$^{-1}$ and 25°C m.y.$^{-1}$ (Figure 5). Slower cooling promotes more extensive grain growth. This, in turn, reduces both the annealing blocking temperature and the maximum temperature at the end of mylonitization. Note, however, that even for a reduction in cooling rate from 125°C m.y.$^{-1}$ to 25°C m.y.$^{-1}$, the reduction in both of these temperatures is only ~20°–30°C. Moreover, grain growth is slower at lower temperatures. Consequently, as the cooling rate tends toward 0°C m.y.$^{-1}$, grain growth is more rapid at a given temperature, but the annealing blocking temperature may be reduced to the point where grain growth is minimal. For example, for 5°C m.y.$^{-1}$ cooling rates appropriate for thrust belts [England and Thompson, 1984], the calculated annealing blocking temperature is only ~30°C less than that for the 25°C m.y.$^{-1}$ cooling rate.

Let us now consider the constraints available on the temperature (T) and differential stress during the deformation of the quartzofeldspathic mylonitic rocks in the Whipple Mountains. As discussed above, grain growth calculations show that temperatures higher than T_{max} result in grain growth that exceeds the observed grain sizes (Figure 5), leaving two possible temperature ranges: either $T_{max}>T>T_a$ or $T<T_a$. If $T_{max}>T>T_a$, then postdeformational grain growth has occurred, and the grain size and inferred differential stress during mylonitization can be read from Figure 5 (maximum values of 100–150 MPa). If $T<T_a$, however, the measured grain size is the same as the grain size during mylonitization, and hence the differential stress can be inferred from the measured grain size (40 and 79 MPa for grain sizes of 55 and 37 μm, respectively). Our calculations do not treat the case where mylonitization may have continued during cooling to lower temperatures, where the rate of dynamic recrystallization was not fast enough to permit the grain size to equilibrate to changes in differential stress, because the requisite experimental data are not available.

ESTIMATES OF STRAIN RATE AND EFFECTIVE VISCOSITY

Once the differential stress has been determined, it can be combined with temperature estimates to determine the strain rate during mylonitization, by using "flow laws," or constitutive relations between stress, temperature, and strain rate. Flow laws are derived from laboratory experiments and in some cases it may be justified to extrapolate them to geologic conditions. If the natural deformation occurs at steady state conditions by the same mechanisms that operated during the experiments (which are generally conducted at higher temperatures and faster strain rates than are appropriate for natural deformations of interest), then the constitutive relations can be used to predict one of the variables, temperature, stress, or strain rate, if the other two variables are known [e.g., Poirier, 1985]. It is preferable to use flow laws of relatively pure quartz rocks, in preference to granitoid rocks, because (1) the quantity we have inferred is the stress supported by the quartz during mylonitization, not the stress supported by a mixture of quartz with feldspar or

other phases, and (2) the rheology of granitoid rocks has been investigated much less comprehensively than that of quartzose rocks. We assume that all rocks in the mylonitic zones were strained at the same rate as the quartz layers so that the strain rate that we infer for the quartz applies to the rock mass. This assumption is probably incorrect because quartz is weaker than feldspar at these conditions [Dell'Angelo and Tullis, 1989], and the quartzose rocks probably deformed at a faster rate than the quartzofeldspathic rocks. Theoretical analysis and experiments on two-phase rocks summarized by Handy [1990] suggest that quartzofeldspathic rocks such as those in the Whipple Mountains [with 20–40% quartz; Anderson et al., 1979] might be as much as five times stronger than pure quartzite.

We did not consider flow laws for vacuum-dried samples, because the presence of biotite and muscovite indicates that the natural samples were not deformed under anhydrous conditions. We have also excluded rheological data from experiments on novaculite and flint. None of the sets of experiments from which the flow laws were derived were ideal [see discussion in Koch et al., 1989]. All were done in solid-medium apparatus, which cannot measure differential stress as accurately as can gas apparatus. Kronenberg and Tullis' [1984] and Jaoul et al.'s [1984] experimental samples were encapsulated in platinum, which affects the stress measurements during the experiments. Further, their rheological data come from creep experiments on five or fewer samples. Koch et al.'s [1989] experiments were done with copper or talc confining media, which are somewhat stronger than the salt confining medium used in some of the other experiments. Although experiments have shown that the rheological behavior of quartz is affected by pressure, impurities such as Na [Jaoul, 1984], water content [Jaoul et al., 1984; Kronenberg and Tullis, 1984], and the α/β transition [Linker and Kirby, 1981; Ross et al., 1983], none of these effects can yet be extrapolated quantitatively to natural conditions.

We calculated strain rates (Table 3) from quartzite flow laws (see Table 5 of Hacker et al. [1990]) for several temperatures (T_{max}, T_a, and 400°C) using the differential stresses derived from the observed grain sizes (Table 2) and the grain growth calculations above (Figure 5). At the annealing blocking temperatures, T_a, the predicted strain rates for the rocks with 37- to 55-μm grain sizes (cooling rate of 125° m.y.$^{-1}$) are in the range 10^{-10} to 10^{-12} s^{-1}. At a lower temperature, 400°C, strain rates are one order of magnitude slower. We prefer the strain rates derived from the experiments of Koch et al. [1989] because they are the most conservative (they are the slowest and yield the slowest exhumation and faulting rates) and because Koch et al.'s "dry" flow law is based on experiments conducted in solid-medium as well as gas-medium [Heard and Carter, 1968] apparatus. Even with the maximum uncertainty (including grain-size variances, piezometer-calibration errors, and flow-law calibration errors), strain rates faster than 10^{-14} s^{-1} are predicted for the mylonitic gneisses deforming at a temperature of 500°C. To convert the strain rates in Table 3 derived from uniaxial compression experiments to shear strain rates it is necessary to express the constitutive relationship in terms of effective shear stress and effective strain rate [Ranalli, 1987, p. 75–79; Schmid et al., 1987, p. 775–776]. For the constitutive relationships used in this study, the shear strain rates are ~1.2–1.4 times the strain rates quoted in Table 3 for uniaxial compression experiments. Note that this means that our previous report on the Ruby Mountains [Hacker et al., 1990] underestimated shear strain rates and displacement rates during faulting by a factor of ~2.6.

An important assumption is that the deformation mechanisms operative during the mylonitization were the same as the deformation mechanisms active during the experiments on which the flow law is based. At least for Koch et al.'s [1989] experiments the deformation microstructures are similar to the Whipple mylonitic rocks—which suggests that the deformation mechanisms were similar, although grain boundary mobility and dislocation recovery may have been greater in the natural samples. Other mechanisms such as grain boundary sliding or diffusive transport could have been active during the mylonitization, however, and may have contributed an unknown amount to the deformation of the rocks.

The midcrustal shear zone in which the gneisses were mylonitized was at least several kilometers thick (based on

TABLE 3. Negative Logarithms of Strain Rates

T(°C)	$\bar{D}$ (μm)	σ(MPa)	Shelton and Tullis (1981)	Hansen and Carter (1982)	Koch et al. (1989) "dry"	Hansen (1982)	Koch et al. (1989) "wet"	Kronenberg and Tullis (1984)	Jaoul et al. (1984)	Logarithm Effective Viscosity (Pa s)
Mylonitic Gneisses With Average Final Grain Size, $\bar{D}$ = 37 μm										
500	20±2	223	$9.9^{+0.4\ +0.5}_{-0.5\ -0.5}$	$8.7^{+0.4}_{-0.4}$	$10.1^{+0.6\ +3.4}_{-0.6\ -3.6}$	$8.2^{+0.4}_{-0.4}$	$9.5^{+0.5\ +2.0}_{-0.6\ -2.1}$	$8.3^{+0.5\ +1.1}_{-0.6\ -2.1}$	$8.9^{+0.3\ +1.6}_{-0.3\ -1.9}$	$18.0^{+0.6\ +3.4}_{-0.6\ -3.6}$
450	37±1	96	$11.2^{+0.4\ +0.4}_{-0.4\ -0.5}$	$9.7^{+0.4}_{-0.4}$	$11.5^{+0.5\ +3.6}_{-0.6\ -3.6}$	$9.5^{+0.4}_{-0.4}$	$10.8^{+0.5\ +2.0}_{-0.6\ -2.1}$	$9.6^{+0.5\ +0.9}_{-0.6\ -1.9}$	$10.0^{+0.3\ +1.5}_{-0.3\ -1.7}$	$19.0^{+0.5\ +3.6}_{-0.6\ -3.6}$
400	37±1	96	$12.1^{+0.4\ +0.4}_{-0.4\ -0.5}$	$10.4^{+0.4}_{-0.4}$	$12.2^{+0.5\ +3.6}_{-0.6\ -3.6}$	$10.4^{+0.4}_{-0.4}$	$11.6^{+0.5\ +2.1}_{-0.6\ -2.2}$	$10.3^{+0.5\ +0.9}_{-0.6\ -2.0}$	$10.8^{+0.3\ +1.5}_{-0.3\ -1.7}$	$19.7^{+0.6\ +3.4}_{-0.6\ -3.6}$
Mylonitic Gneisses With Average Final Grain Size, $\bar{D}$ = 55 μm										
520	27±3	134	$9.8^{+0.4\ +0.5}_{-0.5\ -0.5}$	$8.6^{+0.4}_{-0.4}$	$10.0^{+0.6\ +3.3}_{-0.6\ -3.5}$	$8.0^{+0.4}_{-0.4}$	$9.4^{+0.5\ +2.0}_{-0.6\ -2.1}$	$8.2^{+0.5\ +0.8}_{-0.5\ -1.8}$	$8.7^{+0.3\ +1.5}_{-0.4\ -1.8}$	$17.6^{+0.6\ +3.3}_{-0.6\ -3.5}$
460	55±3	43	$11.7^{+0.4\ +0.4}_{-0.4\ -0.5}$	$10.2^{+0.4}_{-0.3}$	$12.1^{+0.5\ +3.3}_{-0.6\ -3.5}$	$9.8^{+0.3}_{-0.4}$	$11.4^{+0.5\ +1.9}_{-0.5\ -2.0}$	$10.2^{+0.5\ +0.8}_{-0.5\ -1.8}$	$10.3^{+0.3\ +0.13}_{-0.3\ -0\ 15}$	$19.3^{+0.5\ +3.3}_{-0.5\ -3.5}$
400	55±3	43	$12.7^{+0.4\ +0.4}_{-0.4\ -0.5}$	$11.0^{+0.3}_{-0.4}$	$13.0^{+0.5\ +3.5}_{-0.6\ -3.7}$	$11.0^{+0.3}_{-0.4}$	$12.4^{+0.5\ +2.0}_{-0.5\ -2.1}$	$11.0^{+0.5\ +0.8}_{-0.5\ -1.9}$	$11.2^{+0.3\ +1.3}_{-0.3\ -1.5}$	$20.2^{+0.5\ +3.5}_{-0.6\ -3.7}$

Strain rates calculated from the differential stresses given by the piezometer of Koch [1983] and from the temperatures listed in the first column. The uncertainties given are derived from (1) the uncertainty of the stress (first or only +/- numbers) and from (2) the uncertainty of the stress and the uncertainty of the flow-law calibration (second +/- numbers). The effective viscosities were calculated from the slowest strain rate for a given temperature.

Effective viscosity $\eta = \sigma / 3\dot{\epsilon}$ (1 Pa s = 10 poise).

exposures in the Whipple Mountains) and may have been as much as 13 km thick if a seismically reflective zone is correlated with the exposed mylonitic rocks [C.-Y. Wang et al., 1989]. If we assume that the deformation history within this zone involved homogeneous simple shear, then the displacement rate across this shear zone was of the order of centimeters per year, that is, at plate tectonic rates. The Whipple Mountains shear zone does, however, contain packages of unmylonitized rock [Davis, 1988, Figure 10], so the actual displacement rate may have been more rapid.

The effective viscosity during the deformation of the mylonitic rocks, calculated from the estimated stresses and strain rates (Table 3), is $\sim 10^{18\pm3.6}$ Pa s (10^{19} poise) at 500°C and $\sim 10^{20\pm3.6}$ Pa s (10^{21} poise) at 400°C.

DISCUSSION

Comparison With the Ruby Mountains Core Complex

This study in the Whipple Mountains is analogous to a recently published study [Hacker et al., 1990] in the Ruby Mountains, a core complex in northeastern Nevada. Temperatures of mylonitization in the Ruby Mountains, inferred from consideration of quartz grain growth are 450°–500°C. Shear stresses estimated by quartz grain-size piezometry are <50 MPa. Strain rates of 10^{-11} to 10^{-13} s^{-1} were calculated for these temperatures and stresses using experimentally derived quartzite flow laws. Compared to the Whipple Mountains, the grain sizes measured in rocks from the Ruby Mountains suggest that mylonitization occurred at similar temperatures, lower stresses, and slower strain rates. Consequently, the effective viscosity inferred for rocks from the Ruby Mountains is about one order of magnitude greater than for rocks from the Whipple Mountains. These differences are insignificant in view of the uncertainties in the experimental data and the extrapolations involved. It is significant that the stress, strain rates, and effective viscosities derived independently from these two sets of samples and thermochronologic and thermobarometric constraints are similar.

Comparison With Other Studies

Christensen et al. [1989] used the radial variation in $^{87}Sr/^{86}Sr$ ratio in a garnet grown at ~500°C to calculate a strain rate of 5×10^{-14} s^{-1}. This is at least one order of magnitude slower than we have inferred from mylonitic gneisses in the Whipple Mountains. This difference is probably related to differences in the tectonic settings. The garnet grew during nappe emplacement under horizontal contraction in a collision zone, whereas the mylonitization discussed here occurred during horizontal extension.

Christensen et al. [1989] calculated an effective viscosity of 10^{19} Pa s for their garnet-bearing rock by assuming a stress of 0.6 MPa. Sibson [1982] estimated 10^{18}–10^{19} Pa s, for the viscosity of the "quasi-plastic" portion of the San Andreas fault zone. These values are identical to those we have calculated for the Whipple Mountains, and this suggests that viscosities of $\sim 10^{18}$–10^{20} Pa s may be representative of middle crust in a variety of tectonic settings.

Implications for Physical Models of Lithosphere Extension

Seismic-reflection data show that the crust in the Basin and Range province is characterized by numerous reflectors of variable orientation and distribution. The lower crust is highly reflective, and rather continuous reflectors extend from the upper crust as deep as 15–20 km into the mid to lower crust [Allmendinger et al., 1983, 1987]. The reflectors are interpreted to have resulted from a combination of deformation and magmatism [de Voogd et al., 1988; McCarthy and Thompson, 1988]. The continuous reflectors within the lower crust suggest that deformation was fairly homogeneous there, whereas the local presence of rather continuous reflectors that cross from upper to midcrustal levels suggests that much large-scale deformation within the middle to upper crust took place along discrete zones.

The significance of this is that many physical models of the mechanical behavior of the continental lithosphere [e.g., Lynch and Morgan, 1987; Sonder et al., 1987] assume uniform plane strain rate and use a single value for the strength of the lithosphere derived by averaging the vertically integrated yield stress over the thickness of the lithosphere. These models predict strain rates of 10^{-15} s^{-1} [Lynch and Morgan, 1987] or slower, and viscosities of $\sim 10^{21}$ Pa s [Sonder et al., 1987] for extension to form the Basin and Range province. Our measurements suggest that mylonitic midcrustal rocks exposed in the Whipple Mountains formed at strain rates several orders of magnitude faster, with viscosities 1 to 3 orders of magnitude lower. The next generation of physical models that seek to explain the Basin and Range province should treat the continental lithosphere as a spatially heterogeneous medium composed of high-viscosity ($>10^{21}$ Pa s ?), relatively undeformed regions separated by low-viscosity ($\sim 10^{19}$ Pa s), strongly deformed zones.

Future Studies

Data from two core complexes, the Whipple and Ruby Mountains, suggest that conditions of mylonitization were somewhat similar in both mountain ranges. Our estimates of the conditions of mylonitization might possibly be verified by examination of dislocation densities in quartz grains. Thus far, we have used only quartz grain growth kinetic data and quartz grain-size piezometers. An analogous method is to use quartz dislocation-recovery kinetic data and quartz dislocation-density piezometers. Because the activation enthalpy for dislocation recovery in quartz [Christie and Pierce, 1987] is different than that for grain growth of quartz [Pierce and Christie, 1987], it is possible to correct for dislocation recovery and obtain a stress estimate from dislocation densities. Ideally, the stress estimate obtained from a "preannealing" dislocation density should match the stress estimate obtained from a "preannealing" grain size. However, dislocation density may be readily reset by late stress pulses involving quite small strains so that this piezometer is considerably less stable than grain size.

Studies such as this that extrapolate laboratory data to naturally deformed rocks are heavily dependent on the quality and breadth of the laboratory data, and demonstrate the urgent need for further experimental studies. Measurements of the effects of water, pressure, temperature, impurities, and other variables on quartz grain growth rates are needed for more precise determination of grain growth histories in nature. There are many quartzite flow laws available, but most are based on few data. Studies of quartzite rheology that assess the impact of impurities within crystals, the presence of additional phases, and pressure are needed. Only one experimentally calibrated quartz grain-size piezometer is

available; more are required. In addition, calibration of second-order effects involving the aforementioned variables is needed.

SUMMARY

Mylonitic gneisses collected from the Whipple Mountains metamorphic core complex have quartz grain sizes that cluster in the range 32–61 μm. The kinetic laws derived from grain growth data of Tullis and Yund [1982] and Pierce and Christie [1987] indicate that mylonitization must have occurred at or continued to temperatures lower than 500°C. Koch's [1983] quartz grain-size piezometer suggests that the mylonitization occurred at differential stresses of ~40–150 MPa, or maximum shear stresses of ~20–75 MPa. Extrapolation of quartzite flow laws indicates that the mylonitization occurred at strain rates faster than 10^{-14} s^{-1}. These stress and strain rate estimates suggest that during mylonitization, rocks in the fault zone now exposed in the Whipple Mountains had an effective viscosity of ~$10^{18\pm4}$-$10^{20\pm4}$ Pa s at temperatures of about 400°–500°C, respectively. Physical models of the formation of the Basin and Range province would be in greater agreement with seismic reflection data and the strain rates and viscosities presented in this paper if the continental lithosphere were treated as a spatially heterogeneous medium composed of high-viscosity (>10^{21} Pa s ?), relatively undeformed regions separated by low-viscosity (~10^{19} Pa s ?), strongly deformed zones.

Acknowledgments. This project was supported by University of California, Los Angeles, Academic Senate research funds awarded to An Yin. Rob Twiss and Ed DeWitt provided helpful criticism of the manuscript. Helpful discussions regarding the application of mechanical data collected in pure-shear experiments to natural simple-shear deformation were had with Ben van der Pluijm.

REFERENCES

Allmendinger, R.W., J.W. Sharp, D. von Tish, L. Serpa, L. Brown, S. Kaufman, J. Oliver, and R.B. Smith, Cenozoic and Mesozoic structure of the eastern Basin and Range province, Utah, from COCORP seismic-reflection data, *Geology, 11*, 532–536, 1983.

Allmendinger, R.W., T.A. Hauge, E.C. Hauser, C.J. Potter, S.L. Klemperer, K.D. Nelson, P. Knuepfer, and J. Oliver, Overview of the COCORP 40°N transect, western United States: the fabric of an orogen, *Geol. Soc. Am. Bull., 98*, 308–319, 1987.

Anderson, J.L., Core complexes of the Mojave-Sonoran Desert: conditions of plutonism, mylonitization, and decompression, in *Metamorphism and Crustal Evolution of the Western United States*, edited by W.G. Ernst, pp. 503–525, Prentice-Hall, Englewood Cliffs, N.J., 1988.

Anderson, J.L., and M.C. Rowley, Synkinematic intrusion of two-mica and associated granites, Whipple Mountains, California, *Can. Mineral., 19*, 82–101, 1981.

Anderson, J.L., G.A. Davis, and E.G. Frost, Field guide to regional Miocene detachment faulting and early Tertiary(?) mylonitization, Whipple-Buckskin-Rawhide Mountains, southeastern California and western Arizona, in *Geologic Excursions in the Southern California Area*, edited by P.L. Abbott, pp. 109–133, San Diego State University, 1979.

Anderson, J.L., A.P. Barth, and E.D. Young, Mid-crustal roots of Cordilleran metamorphic core complexes, *Geology, 16*, 366–369, 1988.

Bird, P., Continental delamination and the Colorado Plateau, *J. Geophys. Res., 84*, 7561–7571, 1979.

Bird, P., New finite element techniques for modeling deformation histories of continents with stratified temperature-dependent rheology, *J. Geophys. Res., 94*, 3967–3990, 1989.

Bird, P., Lateral extrusion of lower crust from under high topography, in the isostatic limit. *J. Geophys. Res., 96*, 10275-10285, 1991.

Brace, W.F., and D.L. Kohlstedt, Limits on lithospheric stress imposed by laboratory experiments, *J. Geophys. Res., 85*, 6248–6252, 1980.

Carter, N.L., and M.C. Tsenn, Flow properties of continental lithosphere, *Tectonophysics, 136*, 27–63, 1987.

Chen, W.P., and P. Molnar, Focal depth of intracontinental and intraplate earthquakes and their implications for the thermal and mechanical properties of the lithosphere, *J. Geophys. Res., 88*, 4183–4214, 1983.

Christensen, J.N., J.L. Rosenfeld, and D.J. DePaolo, Rates of tectonometamorphic processes from rubidium and strontium isotopes in garnet., *Science, 244*, 1465–1469, 1989.

Christie, J.M., and M.L. Pierce, Dislocation recovery in quartz aggregates during annealing (abstract), *Eos Trans. AGU, 68*, 422, 1987

Coney, P.J., and T.W. Harms, Cordilleran metamorphic core complexes: Cenozoic extensional relics of Mesozoic compression, *Geology, 12*, 550–554, 1984.

Copeland, P., T.M. Harrison, R. Parish, B.C. Burchfiel, K. Hodges, and W.S.F. Kidd, Constraints on the age of normal faulting, north face of Mt. Everest: Implications for Oligo-Miocene uplift (abstract), *Eos Trans. AGU, 68*, 1444, 1987.

Crittenden, M.D., Jr., P.J. Coney, and G.H. Davis, Cordilleran Metamorphic Core Complexes, Mem. Geol. Soc. Am., *153*, 490 pp., 1980.

Davis, G.A., Rapid upward transport of mid-crustal mylonitic gneisses in the footwall of a Miocene detachment fault, Whipple Mountains, southeastern California, *Geol. Rundsch., 77*, 191–209, 1988.

Davis, G.A., and G.S. Lister, Detachment faulting in continental extension: perspectives from the southwestern U.S. Cordillera, Spec. Pep. Geol. Soc. Am., *218*, 133–159, 1988.

Davis, G.A., J.L. Anderson, E.G. Frost, and T.J. Shackleford, Mylonitization and detachment faulting in the Whipple-Buckskin-Rawhide Mountains terrane, southeastern California and western Arizona, in *Cordilleran Metamorphic Core Complexes*, Mem. Geol. Soc. Am., *153*, 79–129, 1980.

Davis, G.A., D.L. Martin, D. Krummenacher, E.G. Frost and R.L. Armstrong, Geologic and geochronologic relations in the lower plate of the Whipple detachment fault, Whipple Mountains, southeastern California:a progress report, in *Mesozoic-Cenozoic Tectonic Evolution of the Colorado River Region, California, Arizona, and Nevada*, edited by E.G. Frost and D.L. Martin, pp. 408–432, Cordilleran, San Diego Calif., 1982.

Davis, G.A., G.S. Lister, and S.J. Reynolds, Structural evolution of the Whipple and South mountains shear zones, southwestern United States, *Geology, 14*, 7–10, 1986.

Dell'Angelo, L.N., and J. Tullis, Fabric development in experimentally sheared quartzites, *Tectonophysics, 169*, 1–21, 1989.

de Voogd, B., L. Serpa, and L. Brown, Crustal extension and magmatic processes: COCORP profiles from Death Valley and the Rio Grande rift, *Geol. Soc. Am. Bull., 100*, 1550–1567, 1988.

DeWitt, Ed., J.F. Sutter, G.A. Davis, and J.L. Anderson, $^{40}Ar/^{39}Ar$ age-spectrum dating of Miocene mylonitic rocks, Whipple Mountains, southeastern California: *Geol. Soc. Am. Abstr. Programs, 18*, 584, 1986.

Dokka R.K., and S.H. Lingrey, Fission track evidence for a Miocene cooling event, Whipple Mountains, southeastern California. in *Cenozoic Paleogeography of the Western United States*, edited by J.M. Armentrout et al., pp. 141–146, Pacific Section of the Society of Economic Paleontologists and Mineralogists, Los Angeles, Calif., 1979.

Dokka, R.K., M.J. Mahaffie, and A.W. Snoke, Thermochronologic evidence of major tectonic denudation associated with detachment faulting, northern Ruby Mountains-East Humboldt Range, Nevada, *Tectonics, 5*, 995–1006, 1986.

England, P.C., and A.B. Thompson, Pressure-temperature-time paths or regional metamorphism, I, Heat transfer during the evolution of regions of thickened continental crust, *J. Pet., 25*, 894–928, 1984.

Frost, E.G., and D.L. Martin (Eds.), *Mesozoic-Cenozoic tectonic evolution of the Colorado River region, California, Arizona, and Nevada*, 608 pp., Cordilleran, San Diego, Calif., 1982.

Frost, E.G., and D.A. Okaya, Regional extent of mid-crustal mylonitic rocks in Arizona and So. California from seismic reflection profiles: distributed simple shear during crustal extension, *Geol. Soc. Am. Abstr. Programs, 19*, 669–670, 1987.

Furlong, K.P., and D.S. Chapman, Thermal state of the lithosphere, *Rev. Geophys., 25*, 1255–1264, 1987.

Gans, P.B., G.A. Mahood, and E. Schermer, Synextensional magmatism in the Basin and Range province. Spec. Pap. Geol. Soc. Am., *233*, 53 pp., 1989.

Goetze, C., Sheared lherzolites: from the point of view of rock mechanics. *Geology, 3*, 172–173, 1975.

Hacker, B.R., The role of deformation in the formation of metamorphic gradients: ridge subduction beneath the Oman ophiolite. *Tectonics*, 10, 455–473, 1991.

Hacker, B.R., A. Yin, J.M. Christie, and A.W. Snoke, Differential stress, strain rate, and temperatures of mylonitization in the Ruby Mountains, Nevada: Implications for the rate and duration of uplift, *J. Geophys. Res., 95*, 8569–8580, 1990.

Handy, M.R., The solid-state flow of polymineralic rocks, *J. Geophys. Res., 95*, 8647–8661, 1990.

Hansen, F.D., Semibrittle creep of selected crustal rocks at 1000 MPa, Ph.D. dissertation, 224 pp., Texas A&M Univ. College Station, 1982.

Hansen, F.D., and N.L. Carter, Creep of selected crustal rocks at 1000 MPa, *Eos Trans. AGU, 63*, 437, 1982.

Harrison, T.M., Diffusion of ^{40}Ar in hornblende, *Contrib. Mineral. Petrol., 78*, 324–331, 1981.

Heard, H.C., and N.L. Carter, Experimentally induced "natural" intragranular flow in quartz and quartzite, *Am. J. Sci., 266*, 1–42, 1968.

Howard, K.A., J.W. Goodge, and B.E. John, Detached crystalline rocks of Mohave, Buck, and Bill Williams Mountains, in *Mesozoic-Cenozoic Tectonic Evolution of the Colorado River Region, California, Arizona, and Nevada*, edited by E.G. Frost, and D.L. Martin, pp. 377–390, Cordillera, San Diego, Calif., 1982.

Hyndman, D.W., and S.A. Myers, The transition from amphibolite-facies mylonite to chloritic breccia and role of the mylonite in formation of Eocene epizonal plutons, Bitterroot dome, Montana. *Geol. Rundsch., 77*, 211–226, 1988.

Jaoul, O., Sodium weakening of Heavitree Quartzite: Preliminary results, *J. Geophys. Res, 89*, 4271–4279, 1984.

Jaoul, O., J.A. Tullis, and A.K. Kronenberg, The effect of varying water contents on the creep behavior of Heavitree quartzite, *J Geophys. Res., 89*, 4298–4312, 1984.

Kanamori, H., The state of stress in the Earth's lithosphere, in *Physics of the Earth's Interior, Enrico Fermi Volume*, edited by A.M. Dziewonski and E. Boschi, pp. 531–554, North-Holland, New York, 1980.

Kirby, S.H., and A.K. Kronenberg, Rheology of the lithosphere, *Rev. Geophys., 21*, 1458–1487, 1987.

Koch, P.S., Rheology and Microstructures of Experimentally Deformed Quartz Aggregates, Ph.D. dissertation, 464 pp., Univ. of Calif., Los Angeles, 1983.

Koch, P.S., J.M. Christie, A. Ord, and R.P. George Jr., Effect of water on the rheology of experimentally deformed quartzite, *J Geophys. Res, 94*, 13975–13996, 1989.

Kronenberg, A.K., and J. Tullis, Flow strengths of quartz aggregates: Grain size and pressure effects due to hydrolytic weakening, *J. Geophys. Res, 89*, 4281–4297, 1984.

Kulik, D.M., and C.J. Schmidt, Region of overlap and style of interaction of Cordilleran thrust belt and Rocky Mountain foreland, *Mem. Geol. Soc. Am.., 171*, 75–98, 1988.

Lachenbruch, A.H., and J.H. Sass, Heat flow in the United States and the thermal regime of the crust, in *The Earth's Crust: Its Nature and Physical Properties, Geophys. Mon, Ser.*, vol. 20, edited by J.G. Heacock, pp. 626–675, AGU, Washington D.C., 1977.

Lee, J., and J.F. Sutter, Incremental $^{40}Ar/^{39}Ar$ thermochronology of mylonitic rocks from the northern Snake Range, Nevada, *Tectonics, 10*, 77–99, 1991.

Linker, M.F., and S.H. Kirby, Anisotropy in the rheology of hydrolytically weakened synthetic quartz crystals, in *Mechanical Behavior of Crustal Rocks, Geophys. Monogr. Ser.*, vol. 24, edited by N.L. Carter et al., pp. 29–48, AGU, Washington D.C., 1981.

Lister, G.S., and G.A. Davis, The origin of metamorphic core complexes and detachment faults formed during Tertiary continental extension in the northern Colorado River region, U.S.A., *J. Struct. Geol., 11*, 65–93, 1989.

Lister, G.S., and A.W. Snoke, S-C mylonites, *J. Struct. Geol., 6*, 617–637, 1984.

Lynch, H.D., and P. Morgan, The tensile strength of the lithosphere and the localization of extension, in Continental Extensional Tectonics, edited by M.P. Coward et al., *Geol. Soc. Spec. Publ. London 28*, 53–65, 1987.

Mainprice, D.H., The Experimental Deformation of Quartz Polycrystals, Ph.D. dissertation, 171 pp., Australian National Univ., Canberra, 171 pp., 1981.

McCarthy, J., and G.A. Thompson, Seismic imaging of extended crust with implications for the western United States, *Geol. Soc. Am. Bull., 100*, 1361–1374, 1988.

McDougall, I., and T.M. Harrison, *Geochronology and Thermochronology by the $^{40}Ar/^{39}Ar$ Method*, 212 pp., Oxford University Press, New York, 1988.

McNutt, M., Lithospheric stress and deformation, *Rev. Geophys., 25*, 1245–1253, 1987.

Mercier, J.-C., D.A. Anderson, and N.L. Carter, Stress in the lithosphere: Inferences from steady-state flow of rocks, *Pure Appl. Geophys., 115*, 199–226, 1977.

Miller, E.L., P.B. Gans, and J. Garing, The Snake Range decollement: An exhumed mid-Tertiary ductile-brittle transition, *Tectonics, 2*, 239–263, 1983.

Molnar, P., and P. England, Temperatures, heat flux, and frictional stress near major thrust faults, *J. Geophys. Res., 95*, 4833–4856, 1990.

Ord, A., and J.M. Christie, Flow stresses from microstructures in mylonitic quartzites of the Moine Thrust zone, Assynt area, Scotland, *J. Struct. Geol., 6*, 639–654, 1984.

Ord, A., and B.E. Hobbs, The strength of the continental crust, detachment zones and the development of plastic instabilities, *Tectonophysics, 158*, 269–289, 1989.

Ord, A., and B.E. Hobbs, Experimental control of the water-weakening effect in quartz, in *Mineral and Rock Deformation: Laboratory Studies—The Paterson Volume, Geophys. Monogr. Ser., vol. 36*, edited by B.E. Hobbs and H.C. Heard, pp. 51–72, AGU, Washington D.C., 1986.

Pierce, M.L., Kinetics of Recovery and Grain Growth in Hydrostatically Annealed Quartz Aggregates, M.S. thesis, 116 pp., Univ. of Calif., Los Angeles, 1987.

Pierce, M.L., and J.M. Christie, Kinetics of grain growth in quartz aggregates (abstract), *Eos Trans. AGU, 68*, 422, 1987.

Poirier, J.-P., *Creep of Crystals*, 260 pp., Cambridge University Press, New York, 1985.

Ranalli, G., *Rheology of the Earth*, 366 pp., Allen & Unwin, Boston, 1987.

Ross, J.V., S.J. Bauer, and N.L. Carter, Effect of the α-β quartz transition on the creep properties of quartzite and granite, *Geophys. Res. Lett., 10*, 1129–1132, 1983.

Schmid, S.M., R. Panozzo, and S. Bauer, Simple shear experiments on calcite rocks: rheology and microfabrics, *J. Struct. Geol., 9*, 747–778.

Sclater, J.G., C. Jaupart, and D. Galson, The heat flow through oceanic and continental crust and the heat loss of the Earth, *Rev. Geophys. Space Phys., 18*, 269–311, 1980.

Shelton, G., and J.A. Tullis, Experimental flow laws for crustal rocks (abstract), *Eos Trans. AGU, 62*, 396, 1981.

Sibson, R.H., Fault zone models, heat flow, and depth distribution of earthquakes in the continental crust of the United States, *Bull. Seismol. Soc. Am., 72*, 151–161, 1982.

Snoke, A. W., and D. M. Miller, Metamorphic and tectonic history of the northeastern Great Basin, in *Metamorphism and Crustal Evolution of the Western United States*, edited by W. G. Ernst, pp. 606–648, Prentice-Hall, Englewood Cliffs, N.J., 1988.

Sonder, L.J., P.C. England, B.P. Wernicke, and R.L. Christensen, A physical model for Cenozoic extension of western North America, in Continental Extensional Tectonics, edited by M.P. Coward et al., *Geol. Soc. Spec. Publ. London, 28*, 187–201, 1987.

Tullis, J.A., and R.A. Yund, Growth kinetics of quartz and calcite aggregates, *J. Geol., 90*, 301–318, 1982.

Twiss, R.J., Theory and applicability of a recrystallized grain size paleopiezometer, *Pure Appl. Geophys., 115*, 227–244, 1977.

Twiss, R.J., Static theory of size variation with stress for subgrains and dynamically recrystallized grains, *U.S. Geol. Surv. Open File Rep., 80-625*, 665–683, 1980.

Twiss, R.J., Variable sensitivity piezometric equations for dislocation density and subgrain diameter and their relevance to olivine and quartz, in *Mineral and Rock Deformation: Laboratory Studies—The Paterson Volume, Geophys. Monogr. Ser., vol. 36*, edited by B.E. Hobbs and H.C. Heard, pp. 247–261, AGU, Washington D.C., 1986.

Valasek, P.A, A.W. Snoke, C.A. Hurich, and S.B. Smithson, Nature and origin of seismic reflection fabric, Ruby-East Humboldt metamorphic core complex, Nevada, *Tectonics, 8*, 391–415, 1989.

Wang, C.-Y., D.A. Okaya, C. Ruppert, G.A. Davis, T.-S. Guo, Z. Zhong, and H.-R. Wenk, Seismic reflectivity of the Whipple Mountains shear zone in southern California, *J. Geophys. Res., 94*, 2989–3005, 1989.

Wang, X., J.G. Liou, and H.K. Mao, Coesite-bearing eclogite from the Dabie Mountains in central China, *Geology, 17*, 1085–1088, 1989.

Wernicke, B.P., Uniform-sense normal simple shear of the continental lithosphere, *Can. J. Earth. Sci., 22*, 108–125, 1985.

Wright, J.E., J.L. Anderson, and G.A. Davis, Timing of plutonism, mylonitization and decompression in a metamorphic core complex, Whipple Mountains, California, *Geo. Soc. Am. Abstr. Programs, 18*, 201, 1986.

Yin, A., Origin of regional, rooted low-angle normal faults: A mechanical model and its tectonic implications. *Tectonics, 3*, 469–482, 1989.

Zeitler, P.K., N.M. Johnson, C.W. Naeser, and R.A.K. Tahirkheli, Fission-track evidence for Quaternary uplift of the Nang Parbat region, Pakistan, *Nature, 298*, 255–257, 1982.

J.M. Christie and A. Yin, Department of Earth and Space Sciences, UCLA, Los Angeles, CA 90024

G.A. Davis, Department of Geology, University of Southern California, Los Angeles , CA 90089

B.R. Hacker, Department of Geology, Stanford University, Stanford CA 94305

(Received September 24, 1990;
revised March 12, 1991;
accepted May 9, 1991.)